Escherichia coli Tryptophanyl-tRNA Synthetase Mutants Selected for Tryptophan Auxotrophy Implicate the Dimer Interface in Optimizing Amino Acid Binding†

Sanja Sever,‡,§ Kelley Rogers,‡,|| M. John Rogers,‡,⊥ Charles Carter, Jr.,# and Dieter Söll*,‡

Department of Molecular Biophysics and Biochemistry, Yale University, New Haven, Connecticut 06520-8114, and Department of Biochemistry and Biophysics, CB #7260, University of North Carolina at Chapel Hill, Chapel Hill, North Carolina 27599-7260

Received September 5, 1995; Revised Manuscript Received October 23, 1995⊗

ABSTRACT: Tryptophan auxotrophs of *Escherichia coli* in which mutations were mapped to the *trpS* locus (encoding tryptophanyl-tRNA synthetase) have been previously isolated. We have investigated the tryptophanyl-tRNA synthetase (TrpRS) purified from six auxotrophic strains for changes in amino acid activation and aminoacylation. Steady-state kinetic analyses show that these mutant TrpRS proteins have increases in the apparent K_M for tryptophan, decreases in turnover number, or both, without significant changes in the apparent K_M for ATP or $tRNA^{Trp}$. The crystal structure of a highly homologous tryptophanyl-tRNA synthetase from *Bacillus stearothermophilus* in a complex with the cognate aminoacyl adenylate allowed us to place the mutations in a structural context. The mutations in the enzymes are located in the KMSKS loop (M196I), in or near the active site (D112E, P129S, A133E) or far from the active site. The last three mutants (T60R, L91F, G329S) could not be predicted by examination of the protein structure as they line an interface between the C-terminal α-helix of one subunit and the Rossmann folds of both subunits, thus affecting a specific region of the dimer interface. These results support a role for dimerization in properly configuring the two active sites of the dimeric enzymes in the Trp/Tyr subclass of class I aminoacyl-tRNA synthetases in order to achieve optimal catalysis.

The accuracy of aminoacylation of tRNA by aminoacyl-tRNA synthetases is a fundamental requirement of protein synthesis. The aminoacylation reaction follows a two-step process: first is the activation of the amino acid leading to formation of an aminoacyl adenylate, and the second is the transfer of the activated amino acid to the terminal ribose of its cognate tRNA. Aminoacyl-tRNA synthetases can be divided into two classes of 10 enzymes each based on conserved sequences (Eriani et al., 1990) and structural motifs (Cusack et al., 1990). All members of class I contain a common loop with the signature sequence KMSKS (Hountondij et al., 1986) and a region of homology with the HIGH peptide (Webster et al., 1984) as part of a Rossmann dinucleotide binding fold of parallel β-sheets (Rossmann et al., 1974). Class II synthetases have an entirely different topology of dinucleotide binding based on antiparallel β-sheets (Cusack et al., 1990, 1991). Extensive studies have provided a detailed understanding of the interactions of these enzymes with their cognate tRNAs (Jahn et al., 1991; Rould et al., 1989). In contrast, the mechanisms by which aminoacyl-tRNA synthetases achieve specificity in recognizing their cognate amino acids are less well characterized, with the exception of TyrRS, whose mechanism has been studied in great detail (Fersht, 1987; de Prat Gay et al., 1993). Generally, recognition and activation of the cognate amino acids have been studied by mutating residues which are predicted to be involved in binding and catalysis based on their evolutionary conservation or their position in the three-dimensional structure of the enzyme in a complex with its cognate amino acid (Fersht, 1987). Studies of this type have been undertaken for tyrosyl- (Wells & Fersht, 1986), methionyl- (Ghosh et al., 1991), and aspartyl- (Cavarelli et al., 1994) tRNA synthetases and can be expected for other synthetases whose crystal structures have recently been solved (Doublié et al., 1995; Nureki et al., 1995).

The traditional strategy of phenotypic selection following random [e.g., Kast and Hennecke (1991)] or saturation mutagenesis can in principle sample a much wider range of variants. The study of such mutants may provide a less biased view of interactions critical for catalysis and may reveal contributions from amino acids whose roles are unlikely to be deduced from examination of the crystal structure. Relevant phenotypes which provided selection strategies for the study of a number of aminoacyl-tRNA synthetases include auxotrophy, temperature sensitivity, and resistance to mechanism-based inhibitors [reviewed in Schimmel and Söll (1979)]. Using classical mutagenic methods, mutants of *Escherichia coli trpS* were isolated several decades ago among tryptophan auxotrophic strains (Bohman & Isaksson, 1978; Doolittle & Yanofsky, 1968; Ito et al., 1968). Growth of these strains could be restored by inclusion of tryptophan in the medium. Preliminary characterization suggested that the mutant enzymes may display a lowered

† This work was supported by grants from the NIH to C.C. and D.S.

* Address correspondence to this author at the Department of Molecular Biophysics and Biochemistry, Yale University, P.O. Box 208114, 266 Whitney Ave., New Haven, CT 06520-8114. Tel: (203) 432-6200. Fax: (203) 432-6202. E-mail: soll@trna.chem.yale.edu.

‡ Yale University.

§ On leave of absence from the Department of Biochemistry, University of Zagreb, Croatia.

|| Current address: Laboratory of Cellular and Developmental Biology, National Institute of Diabetes, Digestive and Kidney Diseases, National Institutes of Health, Bethesda, MD.

⊥ Current address: Laboratory of Parasitic Diseases, National Institutes of Allergy and Infectious Diseases, National Institutes of Health, Bethesda, MD.

University of North Carolina at Chapel Hill.

⊗ Abstract published in *Advance ACS Abstracts,* December 1, 1995.

0006-2960/96/0435-32$12.00/0

affinity for the cognate amino acid. Recently, a crystal structure for a closely related TrpRS from *Bacillus stearothermophilus* has been solved in a complex with the cognate aminoacyl adenylate (Doublié et al., 1995), allowing localization of the mutated residue in the three-dimensional structure. Thus, we cloned these mutant *trpS* genes, isolated the enzymes, and identified the alteration in their kinetic behavior. The results show that a broader spectrum of amino acids is involved in cognate amino acid binding and catalysis than would be predicted by examination of the TrpRS crystal structure.

MATERIALS AND METHODS

General. L-[5-^{3}H]Tryptophan (27 Ci/mmol), L-[3-^{14}C]-tryptophan (53.8 mCi/mmol), and tetrasodium [^{32}P]pyrophosphate (25.87 Ci/mmol) were used in this study. Oligonucleotides were provided by G. O'Neill or purchased from the William M. Keck Foundation for Biochemical Research (Yale University). Purified T7 RNA polymerase was a gift from D. Jeruzalmi. Pfu DNA polymerase was purchased from Stratagene and Sequenase Version 2.0 from USB. $tRNA^{Trp}$ was prepared by *in vitro* transcription with T7 RNA polymerase (Sampson & Uhlenbeck, 1988), using a *Bst*NI digest of the plasmid DNA as previously described (Rogers et al., 1992). tRNA gene transcripts were purified by electrophoresis on denaturing polyacrylamide gels followed by elution (Rogers & Söll, 1993). The unmodified tRNA (lacking the terminal G1) could be acylated as well as wild-type tRNA to 1450 pmol/A_{260} unit. The *in vitro* generated $tRNA^{Trp}$ transcript prepared for this study was aminoacylated by wild-type enzyme with a k_{cat}/K_M value 2.5 times lower than the mature *in vivo* made $tRNA^{Trp}$ (Rogers et al., 1992).

Bacterial Strains and Growth. Mutant and wild-type *trpS* genes were derived from the following strains: *E. coli* W3110 contains the *trpS*$^+$ gene and is the parent for the *trpS*10330 and *trpS*9969 alleles (Hall et al., 1982; Doolittle & Yanofsky, 1968), *trpS*4040 (Ito et al., 1968), and *trpS*271c, *trpS*42c, and *trpS*567c (Bohman & Isaksson, 1978). All mutant strains were auxotrophic for Trp, and the latter three strains were also temperature-sensitive. *E. coli* CJ236 (Kunkel, 1985) was used for *in vitro* mutagenesis, and DH5α was the host strain for cloning.

M9 glucose minimal plates with or without tryptophan (40 μg/mL) were used to test Trp auxotrophy. The temperature-sensitive phenotype of strains *trpS*271c, *trpS*567c, and *trpS*42c was ascertained by growth on M9 glucose minimal plates supplemented with Trp (40 μg/mL) and Arg (40 μg/mL) at 42 °C (nonpermissive temperature) and 30 °C (permissive temperature). *E. coli* auxotrophic strains transformed with recombinant pET3a-*trpS* carrying the mutated *trpS* genes and pGp1-2 plasmids (Tabor & Richardson, 1985) were maintained on M9 minimal plates containing Trp (40 μg/mL), Arg (40 μg/mL), ampicillin (50 μg/mL), and kanamycin (25 μg/mL) as required and were incubated at 30 °C. Overexpression of the cloned enzymes did not restore the growth of the transformed auxotrophic strains on minimal agar plates at temperatures between 30 and 42 °C. For protein purification, the appropriate auxotrophic strain was cultured at 30 °C to a cell density of $A_{600} = 1.0$ in NZCYM medium (Maniatis et al., 1990) containing ampicillin and kanamycin, except 567c which was cultured in M9 minimal medium supplemented with all amino acids (40 μg/mL) except Tyr and Phe which inhibit growth of this strain (Bohman & Isaksson, 1978). Protein expression was induced either by incubating cultures for 30 min at 42 °C or, for temperature-sensitive strains, by addition of nalidixic acid (2 mg/mL in 0.02 M NaOH) to 40 μg/mL (Tabor & Richardson, 1985) followed by growth at 30 °C for 3 h.

Cloning and Construction of the trpS Genes. Each tryptophan auxotrophic strain was the source of genomic DNA from which the *trpS* genes were amplified by PCR (Maniatis et al., 1990) by Pfu DNA polymerase to ensure a low error rate. The oligonucleotides for PCR were based on the *trpS* sequence and contained a *Bam*HI restriction site (in italics) (5′CG*GGATCC*GATGACTAAGCCCATCGTT3′ and 5′CG*GGATCC*TTAACGCTTCGCCACAAAA3′). The amplified fragments were cloned as 1005-bp *Bam*HI pieces containing the entire *trpS* gene into pBR322 and sequenced. For further work one of the *Bam*HI sites was converted to an *Nde*I site. The 1005-bp *Nde*I/*Bam*HI fragments corresponding to the 334 amino acid TrpRS protein were cloned into pET3a expression vectors (Studier et al., 1990). Single point mutations were identified by Sanger dideoxy sequencing of both strands of the cloned trpS genes over the entire coding sequence. Our analysis revealed that *E. coli trpS*9969 contains two mutations: D112E and P129S. To analyze the role of each of these mutations, the single mutations were introduced into the wild-type *glnS*$^+$ gene by site-directed mutagenesis. The nature of the mutated *trpS* genes was confirmed by sequencing; they were recloned as *Nde*I/*Bam*HI DNA fragments into pET3a.

TrpRS Purification. The mutant TrpRS proteins were purified after overexpression of *trpS* genes from pET3a vectors transformed into their original auxotrophic strains to avoid contamination from wild-type enzyme. Each auxotrophic strain was transformed with two compatible plasmids, pGp1-2 for supplying the cell with T7 polymerase (Tabor & Richardson, 1985) and a pET3a vector containing the gene encoding the corresponding mutant TrpRS under the control of the T7 RNA polymerase promotor. The cells were harvested, and the pellet was washed with buffer containing 10 mM Tris-HCl (pH 7.6), 10 mM KCl, 1 mM $MgCl_2$, 10% glycerol, 5 mM DTT, and 0.2 mM PMSF and stored at −80 °C. After thawing, cells were sonicated, and the suspension was centrifuged at 28000*g* for 10 min. The resulting supernatant was centrifuged at 100000*g* for 2 h. Mutant TrpRS enzymes were purified by Mono Q chromatography to electrophoretic homogeneity (as judged by Coomassie Blue staining). The TrpRS proteins were dialyzed for 10 h against buffer containing 100 mM potassium phosphate (pH 7.0), 5 mM $MgCl_2$, 4 mM DTT, 10 mM KCl, and 20% glycerol and stored at −80 °C. Enzyme concentration was determined by active site titration (Fersht et al., 1975) assuming that *E. coli* TrpRS exhibits half-of-the-sites activity (Merle et al., 1986). The most unstable TrpRS enzymes (T60R and A133E) originated from thermosensitive *E. coli* strains.

In Vitro Aminoacylation Assays. These were performed with [^{3}H]tryptophan. To correct for the low counting efficiency of the free [^{3}H]Trp in comparison to that of [^{3}H]-Trp-tRNA, total charging assays with either ^{3}H- or ^{14}C-labeled Trp were performed in parallel so that the conversion factor could be calculated. Assays were performed at 37 °C at pH 7.0 as described (Joseph & Muench, 1971a; Rogers

et al., 1992) in 130 μL reaction mixtures containing 50 mM sodium cacodylate or HEPES buffer (pH 7.0), 10 mM magnesium acetate, 4 mM DTT, and 0.05% BSA. Saturating concentrations were 2 mM for ATP, 2 μM for $tRNA^{Trp}$, and 0.6 mM for Trp (6 μM ^{3}H-labeled amino acid and 594 μM [^{12}C]amino acid). For all kinetic assays the concentrations of ATP, Trp, and $tRNA^{Trp}$ varied over at least a 10-fold range (concentrations for Trp were 2−50 μM when wild-type and *trpS*271c enzymes were assayed and 50−500 μM when other mutant enzymes were assayed). TrpRS concentrations were 0.3−30 nM. Samples were taken in triplicate at 15 s time points and spotted on Whatman 3MM filter disks presoaked in 10 mM unlabeled Trp. The disks were then washed, and radioactivity was measured by scintillation counting (Hoben & Söll, 1985). Kinetic parameters were calculated from Eadie−Hofstee plots; all enzymes obeyed Michaelis−Menten behavior.

PP_i-Exchange Reaction. The conditions were similar to those of the aminoacylation reaction. Assays were preformed at 37 °C at pH 7.0 in 0.2 mL aminoacylation reaction buffer supplemented with 10 mM KF, 10 mM tetrasodium pyrophosphate (specific activity 1 cpm/pmol), 2 mM ATP, and 2 mM Trp when saturating concentrations of ATP and Trp were used. Samples were taken every 15 s and the reaction was stopped by addition of 0.2 mL of a 1% suspension of activated Norite A charcoal in 23% perchloric acid containing 0.3 M sodium pyrophosphate. After dilution with 3 mL of water the mixture was filtered through GF/C disks and then washed five times with water (5 mL) and once with 90% ethanol. The disks were dried and radioactivity was measured. TrpRS concentrations were 20−200 nM. Data analysis was as described above.

RESULTS

Mutations in the E. coli trpS Genes and Their Predicted Location in the B. stearothermophilus TrpRS Structure. Auxotrophic *E. coli trpS* strains were isolated in the 1960's and 1970's (Bohman & Isaksson, 1978; Doolittle & Yanofsky, 1968; Ito et al., 1968.). In order to determine the amino acid substitutions which cause the auxotrophic phenotype, the parent wild-type and six mutant *trpS* genes were cloned by PCR methods and sequenced. Our *trpS*$^+$ gene (GenBank Accession No. U38647) had seven base changes when compared to the published sequence (Hall et al., 1982). Two of these alterations give rise to conservative amino acid changes in positions 30 and 326 (Figure 1). The locations of the six auxotrophic mutations are distributed throughout the *trpS* coding sequence (Figure 1). One of the strains contained a double mutation; from this, the corresponding singly mutated *trpS* genes were constructed (see Materials and Methods).

The crystal structure of the closely related *B. stearothermophilus* TrpRS has been determined (Doublié et al., 1995); thus, a framework to locate mutated amino acids in the structure is available. Figure 1 presents alignments of the bacterial TrpRS sequences (*E. coli*, *Haemophilus influenzae*, *B. stearothermophilus*, and *Bacillus subtilis*). The *B. stearothermophilus* enzyme is six amino acids smaller (328 vs 334 amino acids for the *E. coli* TrpRS). Thus, we identified the corresponding residues in the two proteins by sequence alignment and refer to the mutant sites by giving first the amino acid and position in *E. coli*, followed in parentheses by the corresponding *B. stearothermophilus* information. Identical residues (57% between the *E. coli* and *B. stearothermophilus* enzymes) are distributed evenly throughout the two sequences. There are six blocks of 10 residues within the first 200 amino acids where there are at least nine identities. These include the two consensus sequences, KMSKS and TIGN (more commonly referred to as HIGH), and their neighboring residues, and a segment called the "specificity-determining" helix containing a high proportion of the side chains that interact specifically with the substrate tryptophan. The previously published comparison of structure-based sequence identities between *B. stearothermophilus* TrpRS and the much more distantly related *B. stearothermophilus* TyrRS (Doublié et al., 1995) leaves little doubt that the fold of *E. coli* TrpRS is essentially the same as that of the *B. stearothermophilus* enzyme.

As seen in Figure 1, the mutants can be divided into three groups: mutations in the KMSKS loop (M196I), mutations in or near the active site (D112E, P129S, A133E), and mutations located far from the active site (T60R, L91F, G329S). The last three mutants line the interface between the C-terminal α-helix and an elongated pocket along the surface between the two subunits. We will therefore refer to these three mutants as "interfacial" mutants. The three groups of mutant sites are illustrated in Figure 2, showing their three-dimensional location in the *B. stearothermophilus* TrpRS structure (Doublié et al., 1995).

Steady-State Kinetic Analysis of Mutant TrpRS Enzymes. The kinetic parameters for the wild-type and mutant TrpRS enzymes for all substrates were investigated in aminoacylation and PP_i-exchange reactions (Tables 1 and 2). The determination of the apparent kinetic parameters, k_{cat} and K_M, was made at pH 7.0. The values for the wild-type TrpRS enzyme in the aminoacylation assay are in good agreement with earlier data (Joseph & Muench, 1971a). Likewise, our data on the acylation of the *in vitro* generated $tRNA^{Trp}$ transcript are identical to the previously published data (Rogers et al., 1992). Moreover, each mutation has a similar impact on the steady-state kinetic parameters in both aminoacylation (Table 1) and amino acid activation (Table 2), reinforcing our general conclusions.

Interfacial Mutants: T60R(I58), L91F(A89), and G329S-(G323). Comparison with the high-resolution three-dimensional structure of *B. stearothermophilus* TrpRS (Doublié et al., 1995) indicates that amino acid residues corresponding to threonine at position 60, leucine at position 91, and glycine at position 329 in the *E. coli* sequence are situated rather close to one another at the dimer interface (Figure 2). These are the first dimer interface mutants isolated on the basis of their *in vivo* phenotype for any dimeric class I synthetase. Their kinetic properties are therefore of considerable interest as they may help our understanding of the role of the dimer interface in the TrpRS mechanism.

L91F(A89). Although the amino acid in position 91 is not conserved between *E. coli* and *B. stearothermophilus*, reasonable conclusions can be drawn with respect to the tertiary localization of L91. In *B. stearothermophilus* TrpRS, A89, which corresponds to L91 in the *E. coli* protein, is situated in a helix at the dimer interface two residues behind W91, which is a conserved residue in all four known prokaryotic TrpRS enzymes. Substitution of this leucine with another nonpolar amino acid, phenylalanine, effects the least dramatic change in the dimer interface mutants

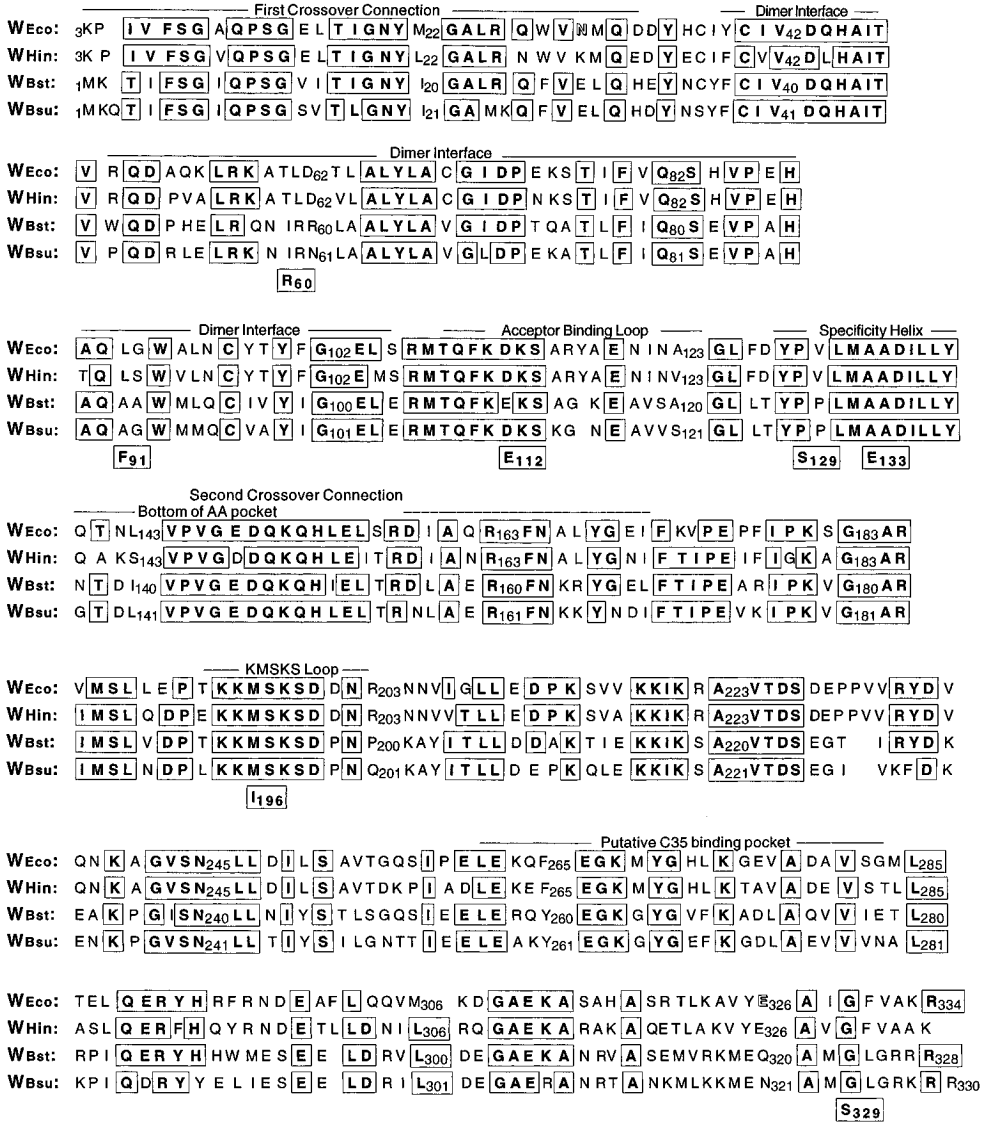

FIGURE 1: *E. coli* TrpRS amino acid sequence has been aligned manually with those of *H. influenzae*, *B. stearothermophilus*, and *B. subtilis* using as a guide the structure-based alignment of TrpRS and TyrRS (Doublié et al., 1995). Mutations identified by sequencing of *trpS* genes from Trp-auxotrophic strains are boxed and situated under the aligned sequences. *E. coli* strain *trpS*9969 contains the D113E and P129S mutations, *trpS*10330 contains the L91F mutation, *trpS*4040 contains the G329S mutation, *trpS*271c contains the M196I mutation, *trpS*42c contains the A133E mutation, and 567c contains the T60R mutation. Positions where our deduced TrpRS amino acid sequence differs from that published earlier (Hall et al., 1982) are N30 and E326. Some of the mutants were temperature-sensitive in addition to being tryptophan auxotrophs.

studied here, and it results in only an approximately 5-fold decrease in the apparent second-order rate constants, k_{cat}/K_M, in both aminoacylation and PP_i-exchange reactions. Whereas in aminoacylation this decrease is due only to a 6-fold increase in the K_M for Trp, the PP_i-exchange reaction shows a 2.7-fold increase in the K_M value for Trp accompanied by approximately a 1.5-fold decrease in turnover rate (Tables 1 and 2). Furthermore, the K_M of this mutant with respect to $tRNA^{Trp}$ is only two times higher compared to wild-type enzyme, and it has a nearly identical K_M with respect to ATP. Among all the mutants studied, the L91F enzyme displays the smallest decrease in the k_{cat}/K_M value.

G329S(G323). G329 corresponds to G323 in the *B. stearothermophilus* TrpRS structure. This is one of the last amino acids that remains ordered in the crystal structure at the end of the C-terminal helix. The G329S mutant enzyme has a decreased k_{cat}/K_M in aminoacylation (0.065) and PP_i-exchange (0.1) reactions compared to wild-type TrpRS (1.0). While in aminoacylation this decrease is entirely due to a 17-fold increase in K_M for Trp, in the PP_i-exchange it is due to a 4-fold increase in K_M and a 2-fold decrease in k_{cat}. Interestingly, as with the other dimer interface mutants, G329S only affects the steady-state parameters of the substrate tryptophan and has minimal impact with respect to those for ATP and $tRNA^{Trp}$.

T60R(I58). The precise location of the T60R mutation is less straight forward to model as it lies in a region with few identities between the *E. coli* and *B. stearothermophilus* sequences. Nonetheless, it can be localized to a region that forms the dimer interface in the *B. stearothermophilus* structure; probably it is structurally equivalent to I58. This residue projects into the dimer interface where it interacts with the preceding mutant, G329(G323). Substitution of the polar threonine residue with a basic arginine residue is the most extreme chemical change among any of our mutants. This enzyme exhibits a 6-fold elevated K_M and a 25-fold decrease in k_{cat}. The K_M value for ATP is almost identical to the wild-type value, and the K_M for the tRNA is only 1.3

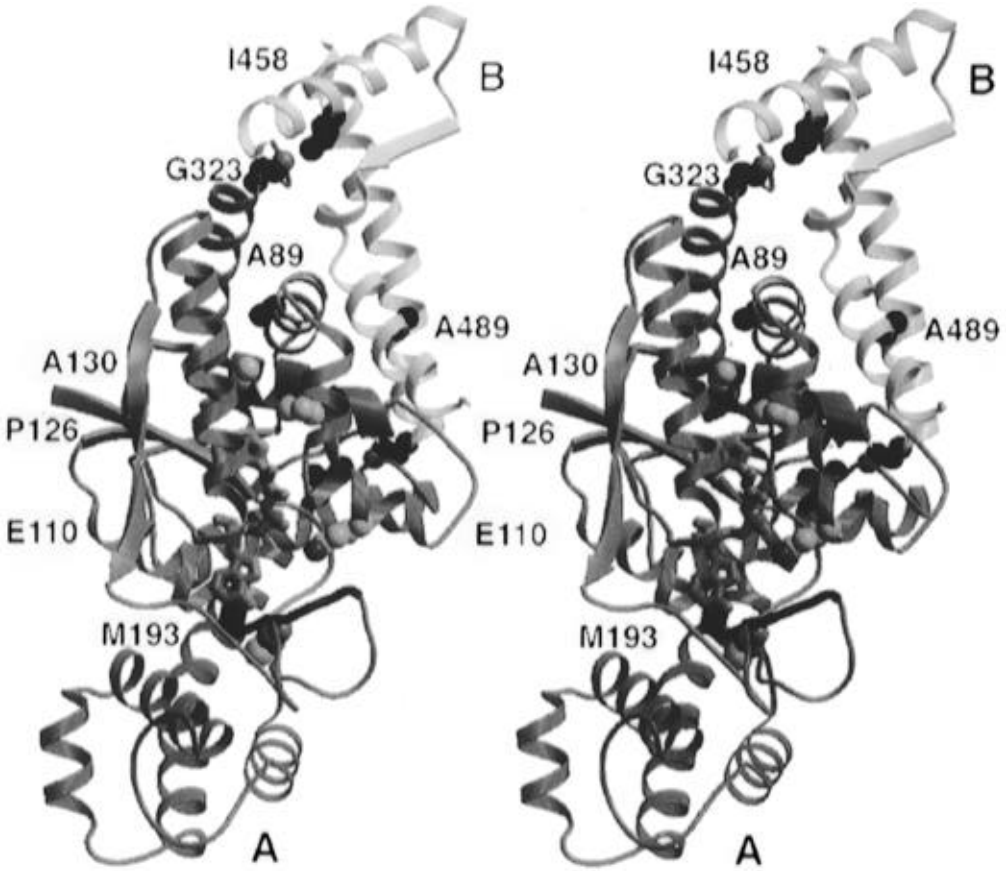

FIGURE 2: Location in the *B. stearothermophilus* TrpRS crystal structure of the mutations identified in this study. One of the two monomers (A) is shown intact in blue, together with the bound ligand tryptophanyl-5′-AMP (green stick drawing), to indicate the active site. The dimer interface region of the other monomer (B) is shown in tan, and residues from this segment are numbered from 401. Segments bounding the active site in monomer A are emphasized, including the TIGN and HIGH consensus sequences (dark blue) and the specificity determining helix (red). Mutant sites are shown by CPK models of their side chains. Three types of mutant sites are suggested by coloring: M196I(M193), in the KMSKS loop, is in red; mutations near the indole binding site [D112E(E110), P129S(P126), and A133E(A130)] are in tan, and the interfacial mutants [T60R(I58), F91L(A89), and G329S(G323)] are in purple.

Table 1: Apparent Kinetic Parameters of the Aminoacylation Reaction

	mutant								
	TrpRS	M196I	L91F	T60R	D112E, P129S	P129S	D112E	G329S	A133E
phenotype	wt	Trp^- t^s	Trp^-	Trp^- t^s	Trp^-	Trp^-	Trp^-	Trp^- t^s	
K_M (Trp) (μM)	12.4 ± 1.2	16.4 ± 1.4	74 ± 7.7	73.2 ± 7.6	114 ± 23	96 ± 9.4	5.8 ± 0.9	215 ± 36	48 ± 4
k_{cat} (Trp) (s^{-1})	2.0 ± 0.2	0.01 ± 0.001	2.4 ± 0.1	0.08 ± 0.003	0.12 ± 0.008	0.10 ± 0.004	2.2 ± 0.26	2.2 ± 0.4	0.6 ± 0.002
rel k_{cat}/K_M	1	0.004	0.199	0.007	0.007	0.006	2.4	0.065	0.072
K_M (ATP) (μM)	190 ± 25	183 ± 30	201 ± 62	161 ± 23	225 ± 8	285 ± 8	216 ± 10	178 ± 67	177 ± 3
k_{cat} (ATP) (s^{-1})	1.5 ± 0.12	0.02 ± 0.002	2.1 ± 0.37	0.1 ± 0.014	0.1 ± 0.002	0.2 ± 0.08	2.2 ± 0.28	1.9 ± 0.36	0.1 ± 0.002
rel k_{cat}/K_M	1	0.014	1.324	0.079	0.056	0.089	1.291	1.352	0.072
K_M (tRNA) (μM)	0.34 ± 0.04	0.27 ± 0.01	0.89 ± 0.01	0.45 ± 0.08	0.56 ± 0.08	0.69 ± 0.16	0.28 ± 0.02	0.65 ± 0.12	0.56 ± 0.08
k_{cat} (tRNA) (s^{-1})	2 ± 0.03	0.02 ± 0.001	2.4 ± 0.18	0.14 ± 0.01	0.11 ± 0.006	0.15 ± 0.02	2.5 ± 0.24	1.05 ± 0.3	0.26 ± 0.02
rel k_{cat}/K_M	1	0.013	0.46	0.053	0.033	0.037	1.5	0.275	0.079
TrpRS stability *in vitro*	stable	stable	stable	very unstable	unstable	unstable	stable	stable	very unstable

times higher than that of wild type. In contrast to other dimer interface mutants, T60R is particularly thermolabile *in vitro*, losing 50% of its activity after a 10 min incubation at 37 °C under the conditions of the aminoacylation and pyrophosphate exchange assays. In the latter assay the TrpRS concentration was 200 nM; thus the loss of activity is probably not due to enzyme subunit dissociation.

Active Site Mutants: D112E(E110), P129S(P126), and A133E(A130). Sequence analysis showed that *trpS*9969 was a double mutant with changes in positions 112 and 129. In the TrpRS crystal structure D112(E110) is positioned in a mobile loop which may interact with the acceptor stem of $tRNA^{Trp}$. However, enzyme kinetics show that TrpRS D112E has enzymatic properties equivalent to those of the wild-type enzyme. Therefore, we deemed it unnecessary to test it in the ATP−PP_i-exchange reaction. We assume that D112E, which is clearly a very conservative mutation, is a silent mutation and not responsible for the phenotype of the double mutant.

P129S(P126). This mutation precedes by two residues a nine amino acid stretch in the specificity-determining helix which is identical in the *E. coli* and *B. stearothermophilus*

Table 2: Apparent Kinetic Parameters during Pyrophosphate Exchange

	mutant							
	TrpRS	M196I	L91F	T60R	D112E, P129S	P129S	G329S	A133E
K_M (Trp) (μM)	18.2 ± 3	23 ± 6	46 ± 1.9	64 ± 11	183 ± 18	200 ± 18	71 ± 9	43 ± 3
k_{cat} (Trp) (s^{-1})	111 ± 7	1.7 ± 0.26	75 ± 1	8.2 ± 1.4	11.8 ± 1.2	13.0 ± 0.8	60 ±	40 ± 11
rel k_{cat}/K_M	1	0.012	0.269	0.02	0.01	0.01	0.14	0.15
K_M (ATP) (μM)	132 ± 9	298 ± 84	194 ± 23	73 ± 15	246 ± 73	281 ± 71	83 ± 8	333 ± 20
k_{cat} (ATP) (s^{-1})	111 ± 8	1.8 ± 0.3	78 ± 6	12 ± 2.5	12 ± 2.2	23 ± 4	37 ± 2	40 ± 2
rel k_{cat}/K_M	1	0.007	0.48	0.196	0.058	0.10	0.531	0.143

TrpRS sequences. As shown in Tables 1 and 2, the kinetic parameters for the single mutant P129S are almost indistinguishable from those of the double mutant. The P129S mutation displays a 10-fold lower turnover rate and a 10-fold higher apparent K_M for Trp. The K_M for ATP is almost identical to that of the wild-type enzyme, and the $tRNA^{Trp}$ value is only 2-fold increased.

A133E(A130). Located about one helical turn beyond P129 in the specificity determining helix, A133E precedes by two residues the conserved D135(D132) which binds to the indole nitrogen of the Trp substrate. The A133→E change leads to a 4-fold increase in the Trp K_M and a 4-fold decrease of the k_{cat}. The K_M values for ATP and tRNA are not changed in the aminoacylation reaction while there is a 2.5-fold increase in the ATP K_M in the ATP−PP_i-exchange reaction.

KMSKS Loop. M196I(M193) represents a relatively conservative change in the KMSKS sequence which nevertheless causes an approximately 100-fold decrease in k_{cat}. There is no effect on the apparent affinity for any of the three substrates in either assay. The large decrease in k_{cat} in the M196I TrpRS enzyme confirms the expected role of the KMSKS motif loop in catalysis (Fersht, 1987; Schmitt et al., 1994).

DISCUSSION

Sequencing of the *trpS* genes from six *E. coli* strains that are auxotrophic for tryptophan revealed that the mutations causing this specific phenotype are distributed throughout the *trpS* coding sequence. Due to the high sequence homology between TrpRS from *E. coli* and *B. stearothermophilus*, whose crystal structure has been solved, it was possible to place the mutations into a structural context. Steady-state kinetic data showed that the mutant enzymes have lower affinity toward tryptophan, a decrease in k_{cat}, or both. Interestingly, some of the mutants studied are located in a specialized region at the dimer interface far away from the active site (Table 3). We attempted to identify pathways through which these residues might communicate with the active site by examination of the enzyme's three-dimensional structure.

Involvement of the Dimer Interface in Binding of Tryptophan. Prior to this work, the production of mutants based on the crystal structure of various aminoacyl-tRNA synthetases identified numerous residues in the active site that are responsible for amino acid binding and activation [e.g., Fersht (1987) and Cavarelli et al. (1994)]. Little was known, however, about interactions elsewhere in the molecule that might significantly contribute to recognition of the cognate amino acid. It was therefore of great interest to identify three TrpRS interfacial mutants that are clustered together in a region that anchors the long C-terminal α-helix against the Rossmann fold (Figure 3). These proteins have substantially lower affinity for tryptophan without significant changes in K_M for ATP or $tRNA^{Trp}$. Since they are all situated at least 14 Å from the active site (Table 3), their effects must be indirect. This finding suggests that the configuration of the dimer interface may be involved in proper positioning of the active site.

Table 3: Distances between the Substrate Tryptophan and Residues in TrpRS *B. stearothermophilus* That Correspond to the Mutated Residues in TrpRS *E. coli*: T60R(I58), L91F(A89), P129S(P126), M196I(M193), and G329S(G323)[a]

C_γ substrate tryptophan to	distance (Å)	primary effect
C_δ58	14.2	k_{cat} 25× decreased, K_M 6× increased
C_β89	12.7*/14.9*	K_M 6× increased
C_δ126	10.5	k_{cat} 20× decreased, K_M 8× increased
C_ϵ193	17.9	k_{cat} 199× decreased
C_α323	28.0	K_M 17× increased

[a] All distances are within the same subunit, with the exception for * where the first interaction is within the monomer and the second across the dimer interface to the opposite active site. Primary effects are determined in the amino acylation assays.

The effects of the interfacial mutations may be caused by their disrupting the packing of the C-terminal helix into the dimer interface. Experimental evidence exists that stability and Trp binding of TrpRS are sensitive to alterations throughout the entire length of the C-terminal helix interface. In *B. stearothermophilus* TrpRS this pocket includes the "methionine zipper" residues (M322, M314, M318, and M93), an interdigitated packing of hydrophobic contacts between the C-terminal helix and the Rossmann fold. This structural feature was implicated in protein stability as substitution of methionine with selenomethionine leads to cold-sensitive enzyme (Doublié et al., 1995). Furthermore, chemical modification of Cys70, situated at the other end of the C-terminal helix, abolishes enzymatic activity (Joseph & Muench, 1971b; Kuehl et al., 1976). This activity can be maintained in the presence of Trp and ATP (Joseph & Muench, 1971b). Although *E. coli* TrpRS does not contain methionine zipper residues, the reduced activity of the G329S enzyme (with the mutation situated near the C-terminus) again points to the importance of the precise positioning of the C-terminus. Substitution of glycine with the larger, polar serine may disrupt this packing and therefore binding of tryptophan to the active site on the opposite subunit. Furthermore, G323, corresponding to the *E. coli* dimer interface mutation G329S, is in van der Waals contact with I58 (T60R) of the other subunit. T60R forms part of an extended pocket that accepts the C-terminus of the other subunit. Since the sequence surrounding G329 in *E. coli* is already rich in basic amino acids, it is possible that the additional positive charge introduced by the T60R mutation

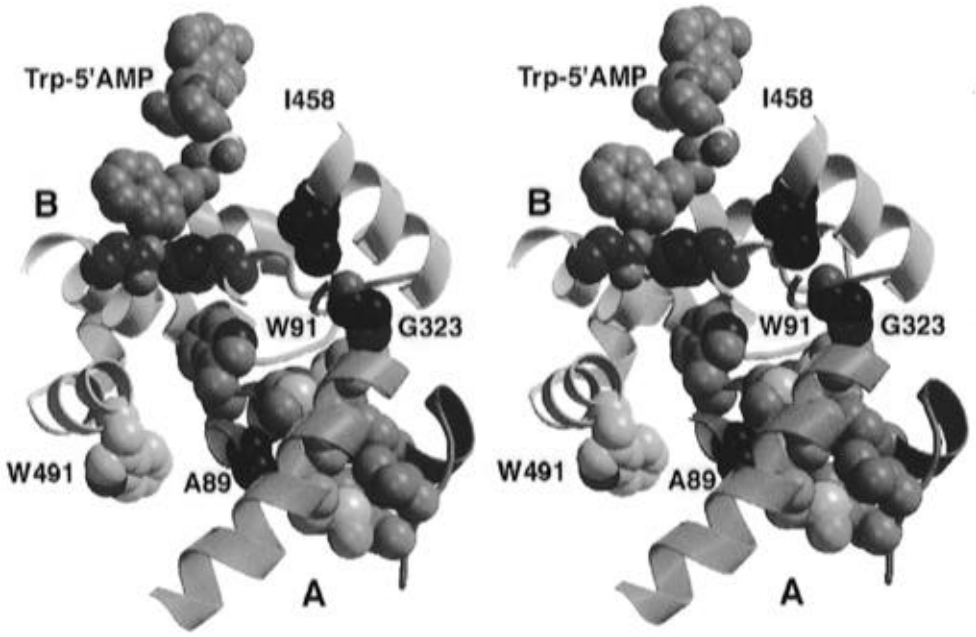

FIGURE 3: Interfacial mutants affecting dimer contacts. Segments of monomer A are in blue; the C-terminal helix is lighter. Those from monomer B are tan and its residues are numbered from 401. Mutant sites are indicated by purple spheres. Other side chains involved in critical contacts include those of the methionine zipper (magenta with yellow sulfur atoms) and H443 and D532 (brown). The molecular 2-fold axes run roughly perpendicular to the figure and between W91 and its symmetry-related mate, W491, near A89.

might destabilize the proper seating of the C-terminus. Furthermore, this local concentration of electrostatic charge provides a reasonable explanation for the thermal instability of this mutant.

L91F Makes Diverse Contacts, Any of Which Could Be Critical for Tryptophan Binding. The mutation lies in an α-helix that forms a major portion of the dimer interface (Figure 3) and projects from this helix against the specificity-determining helix. The substitution involves an increase in the size of the amino acid side chain which could influence tryptophan binding by several mechanisms. Most directly, it might force the specificity-determining helix further into the indole binding pocket, thereby reducing its size. It also might alter the interaction mediated by W93 across the dimer interface. Opposite L91 on the helix is a strictly conserved tryptophan, W93(W91), which penetrates across the dimer interface and into the other indole-binding pocket, interacting with H445 and D532 on the other subunit (Figure 3). Fluorescence measurements on W92 in *B. subtilis* (corresponding to W93 in *E. coli* TrpRS) show a concerted quenching of the W92 fluorescence in the TrpRS·4-fluorotryptophan-AMP complex, strongly suggesting that its environment changes when the activated amino acid is synthesized (Hogue & Szabo, 1993). Displacement of the helix by the L91F mutation could disrupt the hydrogen bond between D532 and the indole nitrogen, decreasing the binding affinity for indole on the opposite subunit. This is analogous to TyrRS where removal of hydroxyl groups of tyrosine residues 34 and 169, which form hydrogen bonds with the substrate tyrosine, does not affect the rate constant for activation but just weakens the binding of tyrosine (Wells & Fersht, 1986). A third possibility is suggested by the series of contacts within the monomer between L91(A89) and amino acids L321(V315) and V324(M318) homologous to those in and near the methionine zipper in the C-terminal helix. Thus, L91F may also disrupt the packing of the C-terminal helix, as described above.

The kinetic behavior of the interfacial mutants suggests that correct packing of the C-terminal helix and dimer interface is critical for proper alignment of the two active sites of some dimeric class I aminoacyl-tRNA synthetases (e.g., TrpRS and TyrRS) in order to achieve optimal catalysis. The integrity of the dimer interface in TyrRS was also shown to be essential for amino acid activation. Jones et al. (1985) found that the mutation F164D in the dimer interface of TyrRS led to reversible dissociation of the TyrRS dimer at high pH. The separated monomers did not catalyze amino acid activation, but the dimer formed at low pH did. Notably, the side chain of F164 in TyrRS occupies a position that nearly superimposes on that of W91 in *B. stearothermophilus* TrpRS.

tRNA Binding to TrpRS. The anticodon is the major identity determinant of $tRNA^{Trp}$ (Himeno et al., 1991; Pak et al., 1992; Rogers et al., 1992); therefore, it has been suggested that binding of $tRNA^{Trp}$ involves recognition sites on both subunits (Doublié et al., 1995). This model was supported by the X-ray structure which showed that the presumptive site for the $tRNA^{Trp}$ anticodon binding and the site of amino acid activation are too close together within a single subunit of the TrpRS dimer to accommodate the large $tRNA^{Trp}$ molecule. Thus it has been proposed that dimerization is essential for $tRNA^{Trp}$ binding. Therefore, we might expect tRNA binding to be adversely affected in some of the interfacial mutants. Surprisingly, all such mutants exhibit on average only a 2-fold increase in the K_M for $tRNA^{Trp}$. Instead, these mutant enzymes show specific effects only on tryptophan binding, which is probably the result of the phenotypic selection used in the isolation of the mutant *E coli* strains. Therefore, we suggest that one role of the dimer interface is in positioning the two active sites in a proper orientation or structure in order to achieve optimal catalysis. A similar model has been proposed for class II aminoacyl-tRNA synthetases (Eriani et al., 1993). Mutations of the highly conserved P273 residues of motif 1 from the

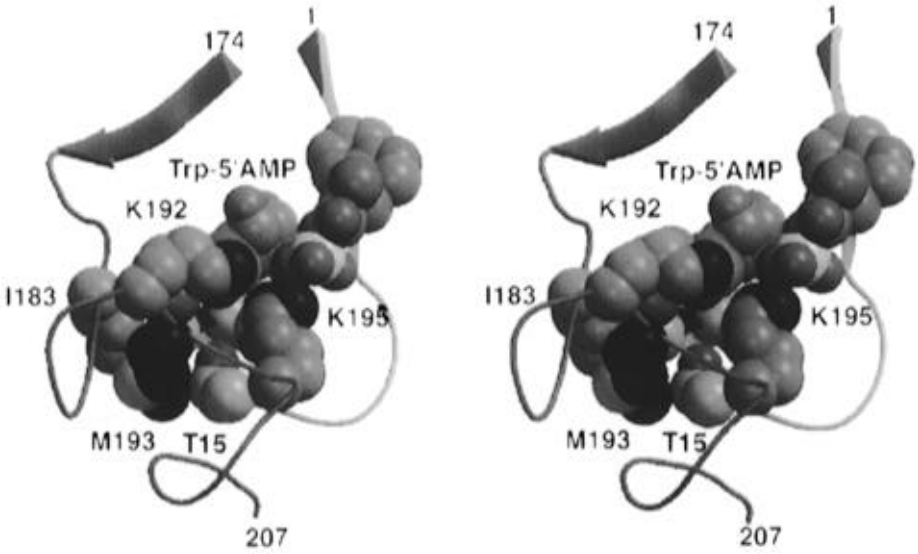

FIGURE 4: Close packing of M193 (purple) against the segment (1−20; tan) containing the TIGN sequence and the activated amino acid. Segments containing the two consensus sequences are colored differently. The TIGN sequence (residues 15−18) is in brown; the KMSKS sequence (192−196) is in dark blue. In the corresponding TyrRS:Tyr−5′-AMP structure, the KFGKS (KMSKS) loop is unfolded by approximately 8 Å away from the active site.

cytoplasmic AspRS from yeast (motif 1 residues form an α-helix involved in the association between subunits) disrupted communication between active sites as seen by steady-state kinetic analysis of AspRS heterodimers. The model is further supported by analysis of the *E. coli* LysRS where a single substitution, T208M in motif 1, induces cooperativity toward amino acid binding (Commans et al., 1995). Although the two different classes of synthetases have completely different topology, our studies of TrpRS suggest a similar role of dimerization in properly configuring active sites in homodimeric class I aminoacyl-tRNA synthetases.

Active Site Mutants: P129S(P126) and A133E(A130). From the crystal structure of the TrpRS·Trp−5′-ATP complex, residues P129 and A133 are situated in the specificity-determining helix that hosts amino acids directly in contact with the indole ring of the tryptophan substrate. Although neither mutated residue is in direct contact with tryptophan, both are in a position to disrupt key interactions between active site residues Y128, M132, and D135 and the indole ring.

The steady-state kinetic data for the P129S mutant support a role for P129(P126) in positioning residues of the specificity helix in order to interact with its indole nitrogen (Doublié et al., 1995). P129 is situated at the N-terminal end of the specificity helix. The P→S replacement could alter the position of the D135 and M132 side chains and hence their ability to form the hydrogen bond or van der Waals bond, respectively, to the indole nitrogen of the substrate.

In contrast to P129S, another active site mutation, A133E, has an overall effect leading to thermal instability of TrpRS. A133(A130) projects from the opposite side of the specificity helix. A→E substitution should certainly destabilize the side-chain packing in the interior of the pocket causing a decrease in affinity toward Trp, while the additional negative charge introduced by the A133E mutation provides a rationale for the thermal instability of the mutant.

Role of Methionine from the KMSKS Motif. Extensive biochemical studies, mainly on TyrRS and recently on MetRS, have shown that residues from the highly conserved KMSKS motif are involved in the formation of the aminoacyl adenylate (First & Fersht, 1993a−c, 1995; Schmitt et al., 1994). The results obtained here with the M196I mutant, which shows a 100-fold decrease in k_{cat}, further support the structural role of methionine in the KMSKS motif (Schmitt et al., 1994). On the basis of the TrpRS crystal structure, the unbranched β-carbon of the methionine side chain, M193, is in close proximity to the side chain of T15, G17, and I183 (Figure 4). The former two residues are the first and third residues of the TIGN consensus sequence. This close association apparently permits the side chains of K192 and K195 to approach the phosphate of that activated amino acid. Examination of this configuration reveals that a side chain branched at the β-carbon, such as isoleucine in the M196I mutant, would be unable to assume this packed configuration without serious steric conflict with neighboring residues T15, G18, and I183. We therefore suggest that in the M196I mutant displacement of the KMSKS loop from this position is sufficient to disrupt the contact made between K195 and the phosphate of ATP, causing a serious reduction of binding affinity to the transition state without altering ground-state affinities.

How Do These Mutant TrpRS Enzymes Lead to Auxotrophy? Vigorous growth requires an ample supply of aminoacyl-tRNA to sustain high rates of protein synthesis, and limitations in aminoacyl-tRNA cause reduction or cessation of growth (Lewis & Ames, 1972; Rojiani et al., 1990). As a matter of fact, it was shown by using the *trpS* strain with the P129S/D112E mutation (see above) that the rate of Trp incorporation into protein is proportional to the amount of Trp-tRNA^{Trp} in the cell (Rojiani et al., 1990). The early characterization in crude extracts of some of the mutant TrpRS enzymes studied here suggested changes in the K_m for the amino acid (Doolittle & Yanofsky, 1968; Bohman & Isaksson, 1978). For all mutants except M196I, the steady-state kinetics presented in this work show a good correlation between the K_M for tryptophan and the requirement for exogenously added Trp to allow growth of the mutant *E. coli* strains. A133E, T60R, and G329S show 4-, 6-, and 17-fold increases in the K_m for Trp, respectively, and

it is possible to rescue their auxotrophic phenotypes at 0.2, 1, and 5 μM concentrations of exogenous Trp, respectively (Bohman & Isaksson, 1978; Ito et al., 1968). For the M196I mutant, tryptophan auxotrophy appears to result from a mutation that affects only the turnover number of TrpRS and not amino acid binding. Among all the mutants studied in this work strain *trpS*271c carrying the M196I mutation requires for growth in minimal medium the lowest amount of tryptophan (0.1 μM; Bohman & Isaksson, 1978). Increasing the tryptophan concentration over the endogenous level probably rescues cells containing the M196I mutation by allowing the mutant TrpRS to work at close to maximum turnover, even though its k_{cat} value is decreased by 100-fold. Therefore, it appears that physiologically higher concentrations of Trp increase the aminoacylation rate of the mutant TrpRS enzymes which have either a high K_M, a low k_{cat}, or both. While it is appealing to see that lowered affinity for tryptophan by TrpRS leads to auxotrophy, strict correlations cannot be made between amino acid binding to the synthetase and the growth rate as this process may be modulated by the complex involvement of Trp-tRNA in protein synthesis and regulation [e.g., Rojiani et al. (1990)].

ACKNOWLEDGMENT

We thank C. Yanofsky (Stanford University) and L. A. Isaksson (Karolinska Institute) for their *trpS* strains and *E. coli* Genetic Stock Center (Yale University) for other strains. We are grateful to Michael Ibba for his critical discussions.

REFERENCES

Bohman, K., & Isaksson, L. A. (1978) *Mol. Gen. Genet. 161*, 285−289.
Cavarelli, J., Eriani, G., Rees, B., Ruff, M., Boeglin, M., Mitscher, A., Martin, F., Gangloff, J., Thierry, J. C., & Moras, D. (1994) *EMBO J. 13*, 327−337.
Commans, S., Blanquet, S., & Plateau, P. (1995) *Biochemistry 34*, 8180−8189.
Cusack, S., Berthet-Colominas, C., Härtlein, M., Nassar, N., & Leberman, R. (1990) *Nature 347*, 203−206.
Cusack, S., Härtlein, M., & Leberman, R. (1991) *Nucleic Acids Res. 19*, 3489−3498.
De Prat Gay, G., Duckworth, H. W., & Fersht, A. R. (1993) *FEBS Lett. 318*, 167−171.
Doolittle, W. F., & Yanofsky, C. (1968) *J. Bacteriol. 95*, 1283−1294.
Doublié, S., Bricogne, G., Gilmore, C., & Carter, C. W., Jr. (1995) *Structure 3*, 17−31.
Eriani, G., Delarue, M., Poch, O., Gangloff, J., & Moras, D. (1990) *Nature 347*, 203−206.
Eriani, G., Cavarelli, J., Martin, F., Dirheimer, G., Moras, D., & Gangloff, J. (1993) *Proc. Natl. Acad. Sci. U.S.A. 90*, 1993.
Fersht, A. R. (1987) *Biochemistry 26*, 8031−8037.
Fersht, A. R., Ashford, J. S., Bruton, C. J., Jakes, R., Koch, G. L. E., & Hartley, B. S. (1975) *Biochemistry 14*, 1−4.
First, E. A., & Fersht, A. R. (1993a) *Biochemistry 32*, 13644−13650.
First, E. A., & Fersht, A. R. (1993b) *Biochemistry 32*, 13651−13657.
First, E. A., & Fersht, A. R. (1993c) *Biochemistry 32*, 13658−13663.
First, E. A., & Fersht, A. R. (1995) *Biochemistry 34*, 5030−5042.
Ghosh, G., Pelka, H., Schulman, L., & Brunie, S. (1991) *Biochemistry 30*, 9569−9575.
Hall, C. V., van Cleemput, M., Muench, K. H., & Yanofsky, C. (1982) *J. Biol. Chem. 257*, 6132−6136.
Himeno, H., Hasegawa, T., Asahara, H., Tamura, H., & Shimizu, M. (1991) *Nucleic Acids Res. 19*, 6379−6382.
Hoben, P., & Söll, D. (1985) *Methods Enzymol. 113*, 55−59.
Hogue, C. W. V., & Szabo, A. G. (1993) *Biophys. Chem. 48*, 159−169.
Hountondij, C., Dessen, P., & Blanquet, S. (1986) *Biochimie 68*, 1071−1078.
Ito, K., Hiraga, S., & Yura, T. (1968) *Genetics 61*, 521−538.
Jahn, M., Rogers, M. J., & Söll, D. (1991) *Nature 352*, 258−260.
Jones, H. D., McMillan, A. J., & Fersht, A. R. (1985) *Biochemistry 24*, 5852−5857.
Joseph, D. R., & Muench, K. H. (1971a) *J. Biol. Chem. 246*, 7602−7609.
Joseph, D. R., & Muench, K. H. (1971b) *J. Biol. Chem. 246*, 7610−7615.
Kast, P., & Hennecke, H. (1991) *J. Mol. Biol. 222*, 99−124.
Kuehl, G. V., Lee, M. L., & Muench K. H. (1976) *J. Biol. Chem. 251*, 3254−3260.
Kunkel, T. A. (1985) *Proc. Natl. Acad. Sci. U.S.A. 82*, 488−492.
Lewis, J. A., & Ames, B. N. (1972) *J. Mol. Biol. 66*, 131−142.
Maniatis, T., Fritsch, E. F., & Sambrook, J. (1990) *Molecular Cloning: A Laboratory Manual*, Cold Spring Harbor Laboratory Press, Cold Spring Harbor, NY.
Merle, M., Trezeguet, V., Graves, P. V., Andrews, D., Muench, K. H., & Labouesse, B. (1986) *Biochemistry 25*, 1115−1123.
Nureki, O., Vassylyev, D. G., Katayanagi, K., Shimizu, T., Sekine, S. I., Kigawa, T., Miyazawa, T., Yokoyama, S., & Morikawa, K. (1995) *Science 267*, 1958−1965.
Pak, M., Pallanck, L., & Schulman, L. H. (1992) *Biochemistry 31*, 3303−3309.
Rogers, K. C., & Söll, D. (1993) *Biochemistry 32*, 14210−14219.
Rogers, M., Adachi, T., Inokuchi, H., & Söll, D. (1992) *Proc. Natl. Acad. Sci. U.S.A. 89*, 3463−3467.
Rojiani, M. V., Jakubowski, H., & Goldman, E. (1990) *Proc. Natl. Acad. Sci. U.S.A. 87*, 1511−1515.
Rossmann, M. G., Moras, D., & Olsen, K. W. (1974) *Nature 250*, 194−199.
Rould, M. A., Perona, J. J., Söll, D., & Steitz, T. A. (1989) *Science 246*, 1135−1142.
Sampson, J. R., & Uhlenbeck, O. C. (1988) *Proc. Natl. Acad. Sci. U.S.A. 85*, 1033−1037.
Schimmel, P. R., & Söll, D. (1979) *Annu. Rev. Biochem. 48*, 601−648.
Schmitt, E., Meinnel, T., Blanquet, S., & Mechulam, Y. (1994) *J. Mol. Biol. 242*, 566−577.
Studier, F. W., Rosenberg, A. H., Dunn, J. J., & Dubendorf, J. W. (1990) *Methods Enzymol. 185*, 60−89.
Tabor, S., & Richardson, C. (1985) *Proc. Natl. Acad. Sci. U.S.A. 82*, 1074−1078.
Webster, T. A., Tsai, H., Kula, M., Mackie, G., & Schimmel, P. (1984) *Science 226*, 1315−1317.
Wells, T., & Fersht, A. R. (1986) *Biochemistry 25*, 1881−1886.

BI952103D